(I/O) Hybrid Alkoxysilane/Zirconium-Oxocluster Copolymers as Coatings for Wood Protection

Simona Maggini,*,[†] Elisabetta Feci,[‡] Elisa Cappelletto,[†] Fabrizio Girardi,[†] Sabrina Palanti,[‡] and Rosa Di Maggio[†]

[†] Dipartimento di Ingegneria dei Materiali e Tecnologie Industriali, Università degli Studi di Trento, via Mesiano 77, 38123 Trento, Italy

[‡]Istituto per la Valorizzazione del Legno e delle Specie Arboree, CNR IVALSA, via Madonna del Piano 10, 50019 Sesto Fiorentino, Italy

S Supporting Information

ABSTRACT: Novel inorganic−organic hybrid copolymers based on vinyl- or (3-mercaptopropyl)-trimethoxysilane and an organically modified zirconium-oxocluster were investigated as a wood preservation treatment. The copolymers were prepared using a modified sol-gel strategy not involving alkoxysilane pre-hydrolysis and were applied on wood through a dip coating method. Even though the copolymers were mainly present on the surface of the wood, EDX analysis showed also a uniform distribution of silicon and zirconium in the cell wall but not in the lumina. The grafting of the copolymers on wood was confirmed through FTIR, ^{13}C and ^{29}Si MAS NMR analysis. The copolymer obtained from (3-mercaptopropyl)trimethoxysilane was post-functionalized with the methacrylic ester of thymol; introduced for testing as a biocide. Preliminary accelerated biological tests against the brown rot fungus *Coniophora puteana*, showed resistance to the fungus for the samples coated with the vinyltrimethoxysilane copolymer, while uneven results were obtained for the samples coated with the (3-mercaptopropyl)-trimethoxysilane copolymer, even when functionalized with the ester of thymol.

KEYWORDS: sol−gel, wood decay, barrier effect, alkoxysilane, (3-mercaptopropyl)-trimethoxysilane, organically modified metal-oxocluster, zirconium oxide
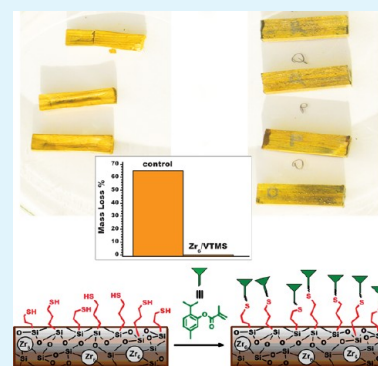
1. INTRODUCTION

An important area of research on wood treatments is controlling or slowing wood destruction due to long-term contact with oxygen, light, moisture and biotic decay.[1−3] Silicon compounds, as a general class, have demonstrated the ability to protect wood from these sources of decay as well as increasing wood's strength and dimensional stability.[4−7] Between the various silicon treatments, one of the most studied involves the application of alkoxysilanes through sol−gel techniques.[8,9]

In the typical sol−-gel process, alkoxysilanes react with water under acidic or basic catalysis, then the formed siloxanes condense to an insoluble gel of polysiloxanes (SiO_x), which can be thermally treated to further increase the condensation/cross-linking. When alkoxysilanes are applied on wood, the water bound to the cell wall can be used to start the sol−gel process. This strategy favors the deposition of the polysiloxane gel inside the cell wall, where the hydroxyl groups of cellulose, hemicelluloses, and lignin can act as binding sites.[10,11] The deposition of the gel in the cell wall is crucial for the improvement of wood properties.[9] Studies have shown that when the hydrolysis is started outside of the wood, the deposition of the gel is mainly in the lumina, resulting in a less effective wood treatment.[8,10]

The alkoxysilane approach to wood protection offers advantages such as the natural abundance of silicon, low cost, low toxicity, and control of hydrolysis. Another approach is the addition of inorganic material in the form of metal oxide,[12−16] which could be incorporated in the wood as addictives in the treatment, or as thin films deposited for example by sol−gel as in the case of titanium oxide,[17−20] which has also shown the capacity to retard the combustion of the wood matrix.

Alkoxysilanes and metal-oxides (aluminum,[21] iron,[22] zirconium,[22] and zinc oxides[23]) have also been used together in inorganic−organic hybrid thin films. These films have shown positive effects on the preservation of the natural color of the wood and stabilization of the wood against sunlight and moisture degradation.

This article explores the application of inorganic−organic hybrid alkoxysilane/zirconium-oxocluster copolymers on wood. The incorporation of zirconium-oxoclusters was aimed at improving the mechanical and thermal resistance of the copolymers.[24]

Organically modified metal-oxoclusters are well-defined objects whose properties can be tuned by varying the metal/organic ligand ratio and the type of organic ligand involved.[25−28] The organic ligands bound to the metal-oxocluster have reactive groups that function as anchoring points to attach the metal-oxocluster to the polymer matrix, allowing a better control of its dispersion. The use of organically modified zirconium-oxoclusters instead of zirconium oxide nanoparticles thus gives a higher versatility and functionality to the copolymers, as well as guaranteeing a better control of the structure and assembly route of the materials.

Specifically, i/o hybrid copolymers obtained from the polymerization of vinyltrimethoxysilane (VTMS) or (3-mercaptopropyl)trimethoxysilane (MPTMS) and the 3-butynoate-substituted zirconium-oxocluster $[Zr_6O_4(OH)_4(OO-CCH_2C\equiv CH)_{12}]_2$ (Zr_6), were considered.

The MPTMS monomer was selected because of the high conversion rates and insensitivity to oxygen inhibition of the thiol-alkyne polymerization, as well as for the antioxidant properties of the thiol groups,[29−31] which could help to protect the wood from photodegradation and fungal decay (free radicals assist fungal decay).[32]

From a previous characterization of the copolymers in bulk,[33,34] it was observed that the copolymers possess unreacted 3-mercaptopropyl or vinyl groups, even when well-formed. These can be used to introduce an extra functionality. This was proven here by photopolymerizing the unreacted 3-mercaptopropyl groups with the double bond of the methacrylic ester of thymol, which was chosen because of the antifungal activity reported by thymol against the fungi: *Poria placenta, Gloeophyllum trabeum, Trametes versicolor, Colletotrichum acutatum, Botryodiplodia Theobromae,* and *Coniophora puteana.*[35−37]

Although the antibacterial and antioxidant activities of thymol are well known,[38−43] the use of thymol as wood preservative has only recently emerged as interest in the use of natural products as biocides has increased,.[44−46] Practical applications of thymol, either as additive in polymer granulate carrier[47] or together as a mixture with other antifungal agents are also reported in patents.[48]

The thymol toxicity towards fungi is not very well understood, but can be considered as a subset of phenolic toxicity, which is based on the inhibition of fungal enzymes containing −SH groups in their active sites.[37,49] However, because the anchoring of thymol to the polysiloxane matrix through an ester group changes the nature of the hydroxyl functional group and the water-solubility and lipophilic properties of the molecule, the antifungal activity of this thymol derivative needs to be tested.[37]

Even without adding a biocide, alkoxysilanes stably bound to wood can enhance resistance against fungal attack.[4,5,50−52] The protection is exerted through hydrophobization of the wood and by modifying the hydroxyl groups of the wood biopolymers through binding. These two actions are both detrimental for the fugal attack which needs a certain amount of water to start and maintain its growth and likewise needs the hydroxyl groups in order to start the attack on cellulose.

After characterization of the coatings on wood, accelerated biological tests against the brown rot fungus *Coniophora puteana,* one of the most aggressive fungi against softwood in Europe, were run in order to determine the efficacy of the protection of the coatings and the antifungal activity of the ester of thymol.

2. EXPERIMENTAL SECTION

2.1. Instrumentation and Methods. Fourier transform infrared spectra (FTIR) were recorded in reflectance mode (ATR system with a zinc selenide crystal) in the range 4000−650 cm^{-1}, using a PerkinElmer Spectrum One instrument. The spectra were recorded with a resolution of 2 cm^{-1} with each spectra averaged over 64 scans. All stack spectra were normalized and baseline corrected before plotting to facilitate easy comparison.

Environmental scanning electron microscopy (ESEM) scans were obtained using a Philips ESEM-TMP XL30 and the microanalysis was conducted using a Falcon-EDAX with a carbon−uranium detector connected to the microscope.

Quantitative analyses on the surface area of the cross section were performed using the standardless method, where the k-ratio is calculated from the measured peak intensity of the elements of interest by using a Pure Element Intensity Factor, and is than corrected by *ZAF* correction factors (matrix correction parameters describing the atomic number effect, the absorption effect, and the fluorescence effect). The analyses were performed with 15 kV or 25 kV acceleration voltages, 1800−1900 CPS, and 50 s counting time.

For the EDX analysis performed on the inner cross section of the coated wood samples, the samples of 30 longitudinal × 10 tangential × 5 radial mm^3 dimension were cut along their cross section to obtain two parts of the same length, using a Struers Minitom equipped with Diamond Cut-off Weel M1D13 (size: 127 mm dia. × 0.4 mm × 12.7 mm dia.), at a speed of 350 rpm.

Solid-state NMR analyses were carried out with a Bruker AVANCE 400 WB instrument equipped with a double resonance 4 mm magic angle spinning (MAS) probe, for ^{29}Si (59.63 MHz) and ^{13}C (75.47 MHz) experiments. Chemical shifts are quoted in parts per million (ppm). Samples were packed in 4 mm-zirconia rotors and spun at 10.0 kHz under air flow for ^{29}Si and ^{13}C analyses. Adamantane and Q_8M_8 were used as an external secondary reference. The conventional T^n notation, where T represents a silicon atom and n the number of bridging oxygen atoms per silicon, was used to describe the ^{29}Si spectra. According to this notation T^0 represented the starting alkoxysilane. The relative amount of T^1, T^2, and T^3 species were determined by integration of the peaks of the ^{29}Si MAS NMR spectra. The degree of condensation (DC) was defined as DC = $\sum_n nT^n/f$, where f is the functionality of the precursor; for VTMS and MPTMS, f = 3.

The photopolymerization was performed using a Helios Italquarz UV lamp, 125W, 230 V, with emission range of 250−450 nm.

Water contact angle measurements were performed through the sessile drop method, using a lab-constructed goniometer for static analyses and a tilting plate method and Cahn 322 microbalance for dynamic analyses. The drop volume of water was 3 μL. The static contact angle was measured with the aid of a digital camera, immediately after the drops deposition. The images were analyzed through Image J software, and contact angle calculations were performed by assuming a spherical approximation of the drop.[53] The equilibrium contact angles were measured using the VIECA (vibrationally induced equilibrium contact angle) method.[54,55]

The wood specimens were cut to be 3.0 cm in length, 1.0 cm in width, and 2 mm in thickness to perform the measurements. The water used for the tests was purified in a Millipore Milli-Q device with UV control, showing a constant electrical resistivity of 18.2 MΩ cm and a surface tension of 72.7 mJ/m^2 at 20 °C. All data were collected at room temperature. Six measurements were performed for each sample. All wood samples were maintained in an oven at 80 °C overnight before the measurements.

2.2. Materials. All commercial reagents and solvents employed were of high-grade purity and were used as supplied without further purification. The anhydrous solvents *n*-propanol 99.7% and tetrahydrofurane (THF) ≥99.9% were purchased from Sigma-Aldrich. The 3-butynoic acid, $[Zr_6O_4(OH)_4(O_2CCH_2C\Xi CH)_{12}]$, and copolymer $Zr_6/$MPTMS/BPO were synthesized according to the procedure in the literature.[33,34] All manipulations were performed under aerobic conditions unless standard Schlenk techniques were required.

4872

dx.doi.org/10.1021/am301206t | *ACS Appl. Mater. Interfaces* 2012, 4, 4871−4881

The wood substrates employed were wood blocks of *Pinus sylvestris* L. sapwood, of dimension 30 longitudinal × 10 tangential × 5 radial mm^3, which were cut from boards with the longitudinal faces parallel to the direction of the grain. On average, the tangential direction of the wood grain intersected the 10 mm face of the samples at an angle between 30 and 45°. The samples had an average of 6−8 annual growth rings per 10 mm. The wood blocks were collected from seven different plants from Val di Susa (Turin, Italy).

2.3. Synthesis of 2-Methylprop-2-enoyl chloride. Methacrylic acid (1.26 g, 14.6 mmol) and thionyl chloride (1.27 ml, 17.5 mmol) in CHCl$_3$ (5 ml) were stirred at 40 °C for 3 h.

2.4. Synthesis of 5-Methyl-2-(propan-2-yl)phenyl 2-methyl-prop-2-enoate (methacrylic ester of thymol). To the previous solution of 2-methylprop-2-enoyl chloride in CHCl$_3$ were added thymol (2.00 g, 13.3 mmol) and NEt$_3$ (4.00 ml, 28.7 mmol). The addition of NEt$_3$ was performed while cooling the system with an ice bath. The resulting solution was stirred at room temperature for 10 h. Toluene was added and the solution was washed with deionised water, then dried on Na$_2$SO$_4$. After filtration of the salt, the solvent was evaporated to recover 5-methyl-2-(propan-2-yl)phenyl 2-methylprop-2-enoate as an oil. The oil was characterized and the results compared with the data reported in the literature.[41] FTIR (ATR): 3060, 3025, 2666, 2926, 2868, 1738, 1719, 1636, 1620, 1585, 1520, 1505, 1484, 1454, 1418, 1380, 1363, 1320, 1291, 1236, 1153, 1127, 1088, 1070, 1060, 1039, 1010, 946, 891, 858, 805, 759, 740, 695, 673. ^{13}C MAS NMR (100.6 MHz): δ = 163.9 (C=O), 150.6 (ArCO), 133.9 ((CH$_3$)C=), 132.9 (ArC), 128.7 (ArC), 124.8 (CH$_2$=), 123.0 (ArCH), 118.1 (ArCH), 113.2 (ArCH), 43.1 (CH(CH$_3$)$_2$), 23.7 (ArCH$_3$), 19.8 (CH(CH$_3$)$_2$), 17.7 ((CH$_3$)C=), 15.1 , 5.2.

2.5. Post-functionalization of Zr$_6$/MPTMS/BPO with the Ester of Thymol. Copolymer Zr$_6$/MPTMS/BPO (0.110 g) was ground into powder. A solution of 5-methyl-2-(propan-2-yl)phenyl 2-methylprop-2-enoate (0.063 g) and IGARGACURE 819 (0.005 g) in CHCl$_3$ (0.2 ml) was added to the powder. The mixture was UV photopolymerized for 1 h, then the solid was washed with CHCl$_3$ and analysed.

FTIR (ATR): 2962, 2928, 2870, 2832, 1746, 1587, 1502, 1487, 1448, 1406, 1340, 1294, 1255, 1240, 1151, 1104, 1061, 1008, 888, 853, 807, 745, 687. ^{13}C CP MAS NMR (100.6 MHz): δ = 229.4 (C=C=C), 220.7 (C=C=C), 172.6 (COO), 161.6 (C=O), 154.5-114.9 (ester of thymol), 76.3 (CH$_2$-C=C=C), 70.0 (C≡CH), 54.9 (CH$_2$), 48.3 (OCH$_3$), 44.2 (CH(CH$_3$)$_2$), 40.0 (CH$_2$), 25.6 (CH$_2$CH$_2$SH), 20.5 (CH(CH$_3$)$_2$), 10.3 (SiCH$_2$).

2.6. Preparation of the Wood Samples before Coatings. Before the coating treatment, each wood sample was oven dried (103 ± 5 °C) for 18 h, in order to determine the anhydrous mass. The samples were then conditioned to constant mass at 20 °C and 65% relative humidity (RH) before applying the coating. Under these conditions the wood reaches equilibrium moisture content at about 12%. The surface of the wood samples of series I and II was then pre-activated by sanding.

The moisture content of the wood samples was confirmed to be around 12% by weighing the conditioned wood samples and referring to their correspondent anhydrous masses (for series III and IV) or drying sacrificial wood samples after their conditioning and sanding (for series I and II).

2.7. Preparation of the Zr$_6$/VTMS/BPO and Zr$_6$/MPTMS/BPO Sol. The sols were prepared by adding to a solution of [Zr$_6$O$_4$(OH)$_4$(OOCCH$_2$C≡CH)$_{12}$]$_2$ (1.075 g) in THF (5.0 ml), vinyltrimethoxysilane (6.2 ml) or (3-mercaptopropyl)trimethoxysilane (7.6 ml) and benzoyl peroxide (BPO, 0.065 g). The stirring was maintained until a clear sol was formed.

2.8. Preparation of the Coated Wood Samples. Four series of coated wood samples were produced (Table 1).

2.8.1. Preparation of the Coated Wood Samples of Series I, II, III. The pine sapwood samples were submerged for 20 mins in the sols described above. The solvent was left to evaporate at atmospheric pressure for 20 mins, then the samples were treated in the oven at 90 °C for 30 min. Each sample was weighed after the dipping, the solvent

Table 1. Series of Coated Wood Samples and the Average Amount of Coating Absorbed

series	type of copolymer	copolymer (g)	no. of samples
I	Zr$_6$/VTMS/BPO	0.074 ± 0.019	4
II	Zr$_6$/VTMS/BPO	0.058 ± 0.024	4
III	Zr$_6$/MPTMS/BPO	0.057 ± 0.012	8
IV	Zr$_6$/MPTMS/BPO	0.050^a ± 0.006	8

^{a}Amount of copolymer and ester of thymol deposited. The amount of ester of thymol for the different samples was in the range 0.006−0.030 g.

evaporation, the thermal treatment and after one day after the treatment.

The amount of coating absorbed by the wood was determined for series I and II by weighing the samples before and after the submersion in the sol, and taking into account the weight percentage of the solvent. For series III and IV, the amount of coating absorbed was determined as the difference between 1) the oven dried mass (103 ± 5 °C, 24 h) of the samples before treatment and 2) the oven dried mass (103 ± 5 °C, 24 h) of the samples after treatment (submersion plus thermal polymerization).

Wood Coated with Zr$_6$/VTMS/BPO. FTIR: 3060, 3024, 2957, 2920, 2852, 1712, 1659, 1603, 1548, 1433, 1410, 1277, 1015, 958, 867, 752 cm^{-1}; ^{13}C CP MAS NMR (75.4 MHz): δ = 172.4 (COO copolymer and carbohydrate), 151.1 (ArCOCH$_3$ lignin), 146.6 (ArCOCH$_3$, ArCOAr, and ArCCH lignin), 134.9 (=CH), 129.5 (=CH$_2$), 118.9-108.3 (ArCH lignin), 103.0 (CHO cellulose), 86.9 (CHO cellulose), 81.8 (CHO cellulose and lignin), 72.32 (CHO lignin and cellulose, CHCH$_2$ cellulose), 69.9 (CHO and CHCH$_2$ cellulose), 60.4 (CH$_2$O lignin), 53.6 (OCH$_3$ lignin), 27.2 (OOCCH$_2$ copolymer), 18.5 (CH$_3$ hemicellulose), 13.6 (CH$_2$ copolymer); ^{29}Si CP MAS NMR (59.6 MHz): δ = -66.4 (0.4 %, [Si(OSi)]), -71.1 (43.5 %, [Si(OSi)$_2$]), -80.2 (56.1 %, [Si(OSi)$_3$]).

Wood Coated with Zr$_6$/MPTMS/BPO. FTIR: 3293, 2928, 2891, 2844, 2565, 1656, 1586, 1423, 1407, 1344, 1307, 1260, 1239, 1185, 1072, 1015, 954, 924, 861, 801, 720, 688 cm^{-1}; ^{13}C CP MAS NMR (75.4 MHz): δ = 101.8 (CHO cellulose), 85.7 (CHO cellulose), 80.7 (CHO cellulose and lignin), 71.2 (CHO lignin and cellulose, CHCH$_2$ cellulose), 68.7 (CHO and CHCH$_2$ cellulose), 61.5 (CH$_2$O lignin), 54.3 (OCH$_3$ lignin), 46.3, 24.4 (CH$_2$CH$_2$SH and CH$_2$SH copolymer), 18.2 (CH$_3$COO hemicellulose), 14.5 (SiCH$_2$ copolymer), 8.5; ^{29}Si CP MAS NMR (59.6 MHz): δ = −48.9 (6.1 %, [Si(OSi)]), −57.5 (40.1%, [Si(OSi)$_2$]), −66.8 (53.8 %, [Si(OSi)$_3$]).

2.8.2. Preparation of the Coated Wood Samples of Series IV. Wood samples coated with copolymer Zr$_6$/MPTMS/BPO (as series III) were treated with a film of 5-methyl-2-(propan-2-yl)phenyl 2-methylprop-2-enoate (0.935 g, 4.28 mmol) and IGARGACURE 819 (4 % in weight respect to the ester of thymol).

The film was applied with a brush on half of the samples, while for the other half the same film but diluted with CHCl$_3$ (3.5 ml) was applied by submersion of the samples for 20 mins in the solution. The application of the film by brush deposited a higher amount of ester of thymol on the samples (around 30 mg). After the deposition of the films all the samples were UV photopolymerized for 1 h. FTIR: 3057, 2964, 2928, 2871, 1742, 1706, 1666, 1610, 1572, 1505, 1486, 1454, 1438, 1416, 1381, 1364, 1343, 1279, 1259, 1238, 1135, 1069, 1057, 1039, 1023, 1001, 924, 890, 852, 817, 750, 713, 695, 668 cm^{-1}.

2.9. Biological Test against Fungal Decay. *2.9.1. Leaching.* Before the biological test the coated wood samples were subjected to leaching according to EN 84 (1997).[56]

Wood specimens were placed in a glass beaker filled with deionised water conforming to EN ISO 3696 (1996) and prevented from floating by the use of weights. The beaker was put in a desiccator and vacuum corresponding to a residual pressure of 4 kPa was applied and maintained for 20 minutes, and then released to return to normal pressure. Wood specimens were maintained in water (ratio of water to wood 5:1) for 14 days with 9 water changes, and then conditioned to constant mass.
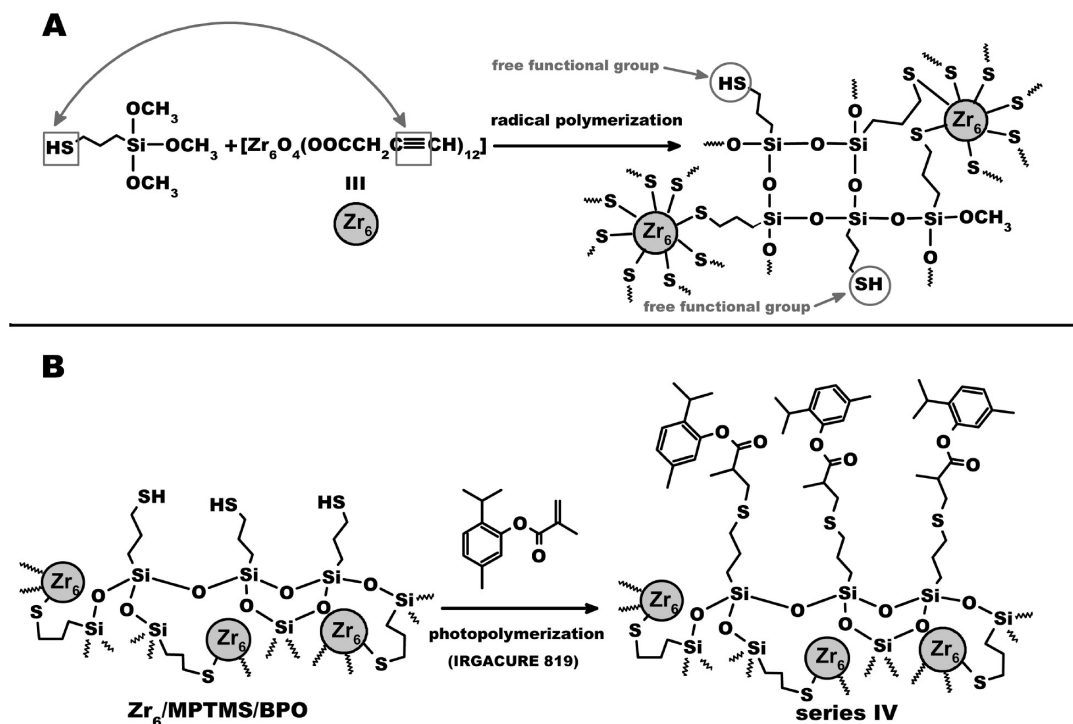
Figure 1. (A) Schematic representation of the synthesis and structure of the Zr_6/MPTMS/BPO copolymer. (B) Schematic representation of the photopolymerization of the methacrylic ester of thymol with the samples coated with Zr6/MPTMS/BPO, performed using IGARGACURE 819 as photoinitiator.

For series III and IV, the weight loss percentage (WL_l%) after leaching was calculated according to eq 1:

$$WL_l\% = \frac{M_t - M_l}{M_0} \times 100 \tag{1}$$

where M_l and M_t are the oven dry (103 ± 5 °C, for 18 h) masses of the samples prior (M_t) and after leaching (M_l), and M_0 is the oven dry (103 ± 5 °C, for 18 h) mass of the untreated wood samples.

The percentage of formulation that leached out during water immersion was calculated according to eq 2:

$$LF\% = \frac{M_t - M_l}{M_t - M_0} \times 100 \tag{2}$$

2.9.2. Efficacy Test against the Brown Rot Fungus Coniophora puteana. Biological tests against the brown rot fungus *Coniophora puteana* were run on the coated wood sample series.

An accelerated mini-block test was employed in order to investigate the efficacy of the coatings. This test, which exposes pine sapwood mini-blocks to the fungus for a period of 6–8 weeks, was proved by Bravery[57] to lead to toxic values comparable with those obtained after 12 weeks using sample sizes described in EN 113,[58] and thus was preferred for a preliminary screening. Untreated pine sapwood mini-blocks were used as controls to check the fungal virulence.

Before exposure to wood specimens, the brown rot fungus *Coniophora puteana* (Schumacher ex Fries) Karsten, strain BAM Ebw. 15 was grown on 80 mL of 4% malt and 2.5% agar medium inside Kolle flasks.

The treated samples (4 or 8 replicates) were then placed in an inoculated Kolle flask together with the untreated reference samples. The wood blocks were incubated with the fungus for six to eight weeks at 22 °C and 75% RH. The resistance was evaluated through the measurement of the mass loss of wood, which was calculated for each individual block as the difference between the dry mass before and after the fungal exposure (eq 3):

$$ML\% = \frac{M_{0before} - M_{0after}}{M_{0untreated}} \times 100 \tag{3}$$

3. RESULTS AND DISCUSSION

The coatings were prepared through a modified sol-gel process[59,60] not involving trialkoxysilane pre-hydrolysis in order to facilitate the deposition of the polysiloxane matrix, obtained from vinyltrimethoxysilane (VTMS) or (3-mercaptopropyl)trimethoxysilane (MPTMS), in the wood cell wall. After the evaporation of the solvent, the samples were thermally treated at 90 °C to activate the radical polymerization between the alkyl chains of the polysiloxane matrix and $[Zr_6O_4(OH)_4(OOCCH_2C{\equiv}CH)_{12}]$ (Zr_6), and form the copolymers. Higher temperatures were not used to avoid the decomposition of the organic components of the wood.

The structure of the formed copolymers consisted of a polysiloxane matrix derived from the condensation of VTMS or MPTMS and 3-butynoate-substituted zirconium-oxoclusters bound to the matrix through C–C or C–S bonds created by radical polymerization of the C≡C or SH groups of the polysiloxanes with the triple bond of the 3-butynoate ligands (Figure 1A).

In total, four series of coated wood samples were produced by dip coating. Series I and II were both obtained with copolymer Zr_6/VTMS/BPO, but in series II the dipping in the sol and the thermal treatment were repeated twice, in order to obtain a double layer of coating. Series III and IV were obtained with copolymer Zr_6/MPTMS/BPO. Series IV was prepared by applying a film of the methacrylic ester of thymol on the samples coated with Zr_6/MPTMS/BPO and photopolymerizing using an UV-lamp (Figure 1B).

The UV photopolymerization conditions were optimized during prior tests performed directly on the copolymer Zr_6/MPTMS/BPO powder. FTIR and ^{13}C MAS NMR were employed to monitor the completeness of the reaction and characterize the outcome, as reported in Figures 2 and 3. The presence of the C=O and C=C bands and the decrease of the
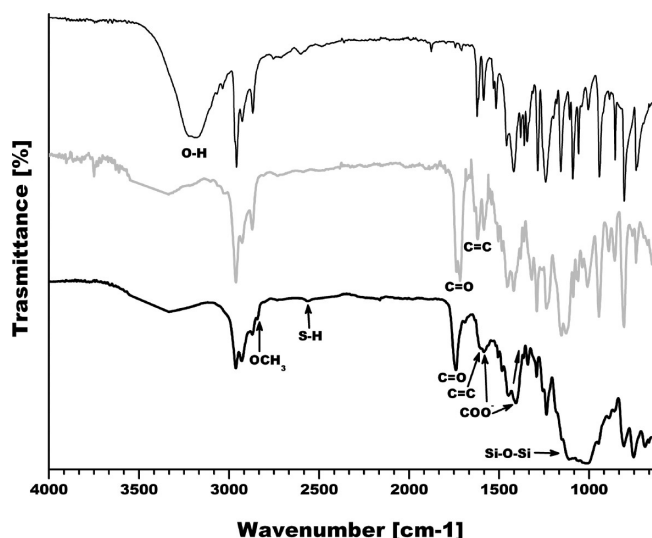
Figure 2. FTIR of thymol (thin black line), methacrylic ester of thymol (gray line), and Zr_6/MPTMS/BPO copolymer functionalized with the ester of thymol (bold black line).
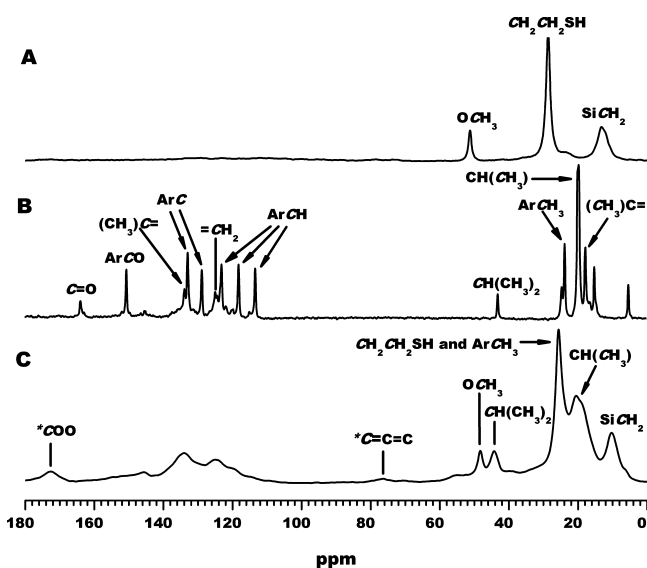
Figure 3. ^{13}C MAS NMR of (A) the Zr_6/VTMS/BPO copolymer, (B) methacrylic ester of thymol, and (C) Zr6/VTMS/BPO functionalized with the ester of thymol; * = signals derived from the 3-butynoate ligands bound to the zirconium-oxoclusters.

S−H band in the FTIR spectrum (Figure 2, bold black line) together with the presence of the $CH(CH_3)_2$ and C aromatic signals in the ^{13}C MAS NMR spectrum (Figure 3C) were considered an indication of the success of the reaction.

The coatings were transparent and did not visibly alter the colour of the wood. FTIR, NMR and EDX analysis of samples of series I and III, which were chosen as representative of all the sample's series, confirmed the grafting of the copolymers to the wood.

ESEM analysis showed a uniform distribution of the coatings and no cracks on the surface (Figure 4), indicating that the coating was not too brittle and did not manifest excessive shrinkage after the thermal treatment. A microanalysis of the coatings, performed by EDX showed also a homogeneous distribution of the zirconium and silicon inside the coating (Figure 4), which implies, as should be expected, the formation

of a stable bond between the zirconium-oxoclusters and the polymer matrix.

From EDX analyses performed on the inner cross section of the samples measured at different depths across the 5 mm dimension, it was observed that the bulk of the coatings remained on the surface (Table 2 Si/C ratio), which was expected given that the sample was dip coated. At a distance of 10 μm from the surface, the amount of silicon in the samples of series II and III had decreased respectively 5 and 16 times compared to the surface. Atomic percentage measurements, performed until 2000 μm (the half point is 2500 μm) showed that a Zr to Si ratio of 1 to 10 was roughly maintained at different depths.

From element mapping (Figure 5), a mostly homogeneous distribution of zirconium and silicon was observed on the entire inner cross section though in a low concentration.

ESEM/EDX showed also that only a scarce amount of the copolymers were present in the inner cell walls and that the lumina were not filled.

FTIR analyses were performed in reflectance mode, involving a 0.3−3 μm penetration depth of the incident radiation according to the wavelength of light, the angle of incidence, and the medium.

The spectra (Figures 6 and 7, grey line) of fragments obtained from the surface of the coated wood samples showed the peaks of the copolymers together with the cellulose, hemicellulose, and lignin[61] peaks in the background.

For the wood samples coated with Zr_6/VTMS/BPO, the bands of the copolymer were observed at: 3060 and 3024 cm^{-1} for =CH$_2$ and =CH stretching, 2957 and 2920 cm^{-1} for CH$_2$ and CH$_3$ stretching, 2852 cm^{-1} for OCH$_3$ stretching, and 1548 and 1433 cm^{-1} for O−C=O stretching. For the wood coated with Zr_6/MPTMS/BPO, at: 3293 cm^{-1} for ≡C−H stretching, 2928 and 2891 cm^{-1} for CH$_3$ and CH$_2$ stretching, 2844 cm^{-1} for OCH$_3$ stretching, 2565 cm^{-1} for S−H, 1586 and 1423 cm^{-1} for O−C=O stretching. For both samples, the band at 1015 cm^{-1} of the Si−O−Si stretching was broadened by C−O stretching of the biopolymers and the OCH$_3$ stretching band was still present, indicating that not all the Si-OCH$_3$ groups of the copolymers on the surface were reacted. Since in a sol−gel process the hydrolysis of alkoxysilanes never reaches completion even when an excess of water is added, the presence of Si-OCH$_3$ groups in the spectra of the fragments obtained from the surface of the coated wood samples can be easily explained, considering also that in our case the hydrolysis was initiated by the moisture content of the wood.

In the FTIR spectra of the inner section of the samples (Figures 6 and 7, bold black line), the peaks of the wood components were prevalent, in agreement with a low concentration of the copolymers. However, a reduction of the O−H band compared to the spectrum of the untreated wood, which was more visible for the sample coated with Zr_6/VTMS/BPO, was noticed.

Similarly, ^{13}C MAS NMR analyses showed the typical signals of the wood components[62] together with the peaks of the copolymers and confirmed that the modified sol−gel process didn't damage the wood or the structure of the copolymers inside it.

^{13}C MAS NMR of the wood coated with Zr_6/VTMS/BPO (Figure 8) showed the peaks of the copolymer at: 172.4 (COO), 134.9 (=CH), 129.5 (=CH$_2$), 27.2 (OOCCH$_2$), and 13.7 (CH$_2$) ppm which belong to the vinyl groups of the siloxanes and the carboxyl and methylene groups of the 3-

4875

dx.doi.org/10.1021/am301206t | ACS Appl. Mater. Interfaces 2012, 4, 4871−4881
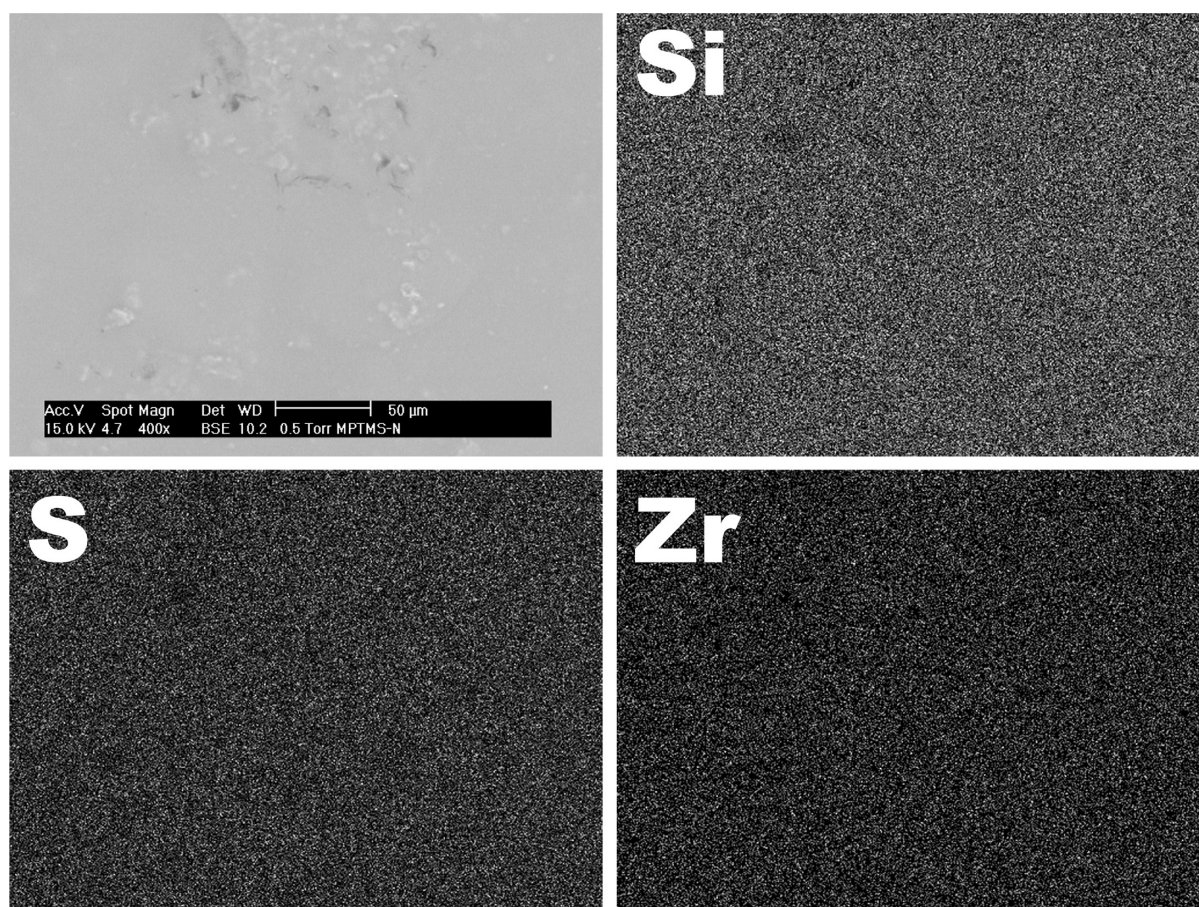
Figure 4. ESEM of the surface of the wood sample coated with Zr_6/MPTMS/BPO and its silicon, sulphur, and zirconium mapping.

Table 2. EDX Standardless Analysis[a]

coating	depth (μm)	C %	Si %	Zr %	S%	Si/C	Zr/Si
Zr_6/VTMS/BPO	surface	74.89 (1.25)	19.91 (0.50)	2.13 (1.63)		0.27	0.1
	10	95.68 (0.72)	3.97 (0.75)	0.36 (2.80)		0.04	0.1
	80	99.85 (0.64)	0.80 (2.12)	0.07 (10.39)		0.008	0.1
	160	99.73 (0.63)	0.26 (4.80)	0.01 (41.67)		0.003	0.04
	500	99.66 (0.63)	0.32 (3.99)	0.03 (24.28)		0.003	0.1
	1000	99.68 (0.64)	0.29 (4.62)	0.03 (32.26)		0.003	0.1
	2000	99.68 (0.64)	0.27 (4.68)	0.04 (14.17)		0.003	0.2
Zr_6/MPTMS/BPO	surface	77.01 (1.74)	11.38 (0.83)	2.42 (1.78)	11.22 (0.90)	0.15	0.2
	10	98.60 (0.64)	0.70 (2.15)	0.05 (11.03)	0.67 (1.97)	0.007	0.1
	80	99.35 (0.65)	0.31 (4.18)	0.03 (26.27)	0.31 (3.61)	0.003	0.1
	160	99.80 (0.64)	0.10 (10.99)	0.01 (58.92)	0.09 (10.23)	0.001	0.1
	500	99.86 (0.6)	0.07 (13.29)	0.01 (36.68)	0.06 (14.01)	0.001	0.1
	1000	99.87 (0.57)	0.06 (16.34)	0 (112.63)	0.06 (11.30)	0.001	-
	2000	99.85 (0.59)	0.06 (17.09)	0 (0)	0.1 (8.82)	0.001	-

[a]Relative atomic percentages of carbon, silicon, and zirconium obtained by EDX standardless analyses on the surfaces and on the inner cross-sections of the coated wood samples with copolymer Zr_6/VTMS/BPO or Zr_6/MPTMS/BPO. The values in parentheses are the intensity errors expressed as a percentage of the atomic percentage.

butynoate ligands. The observation of the $=$CH and $=$CH$_2$ peaks confirmed that not all the vinyl groups were reacted. No SiOCH$_3$ carbon was visible in the spectrum, indicating that inside the wood these groups of the copolymer were probably hydrolysed and reacted with the hydroxyl groups of the wood to form Si$-$O$-$C$_{wood}$ bonds, in agreement with the reduced O$-$H band in the FTIR analysis.

Because of the lower amount of copolymer present on the wood coated with Zr_6/MPMS/BPO, the ^{13}C MAS NMR

(Figure 9) showed mainly peaks due to the wood components and only small peaks assigned to the copolymer at 14.5 (SiCH$_2$), and 24.4 (CH$_2$CH$_2$SH).

The ^{29}Si MAS NMR confirmed the presence of silicon in the sample and the formation of the polysiloxane matrix, since the T^1 [Si(OSi)], T^2 [Si(OSi)$_2$], and T^3 [Si(OSi)$_3$] signals were present. The degree of condensation (DC) of the copolymers inside the wood, which was evaluated through the integration of the T^n signals, had high values (0.85 for Zr_6/VTMS/BPO

4876

dx.doi.org/10.1021/am301206t | ACS Appl. Mater. Interfaces 2012, 4, 4871−4881
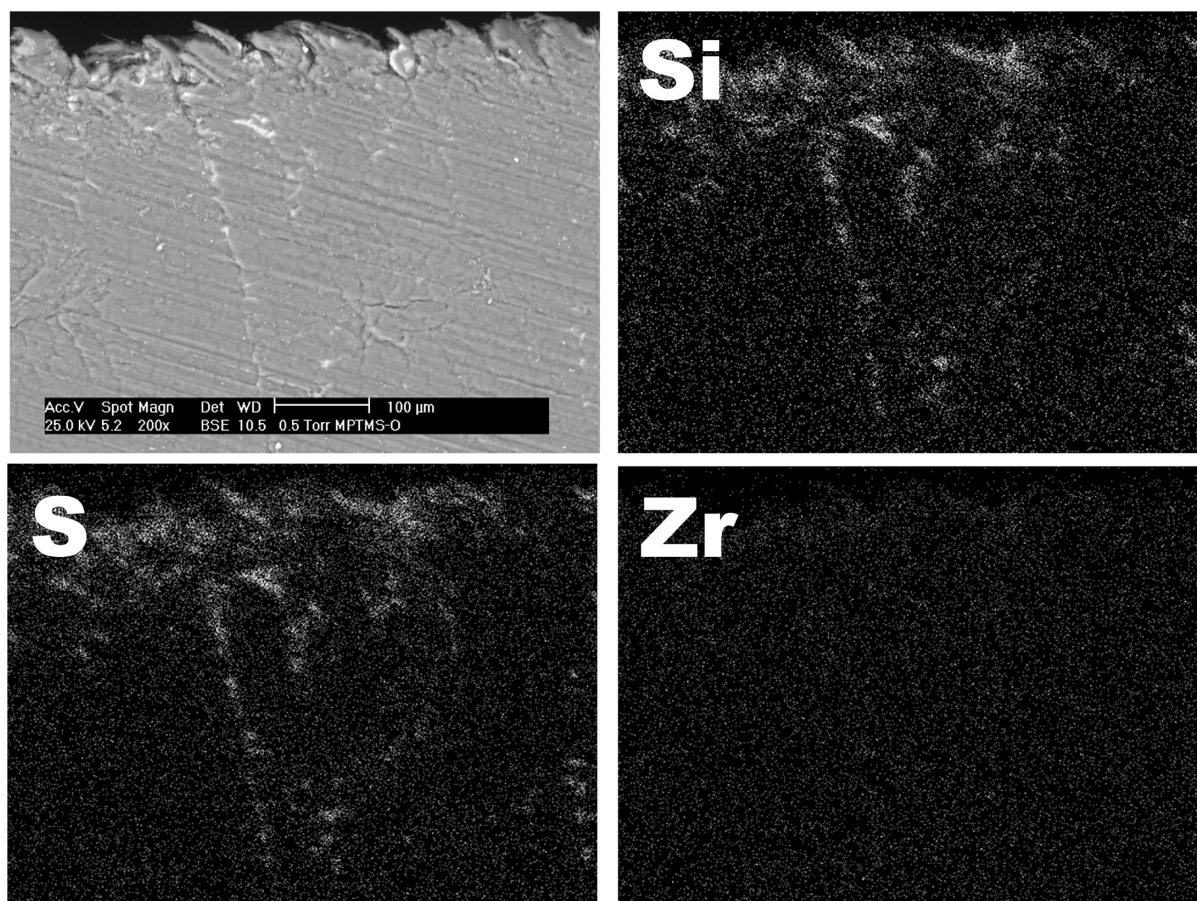
Figure 5. ESEM of the inner cross-section of the wood sample coated with Zr_6/MPTMS/BPO and its silicon, sulphur, and zirconium mapping.
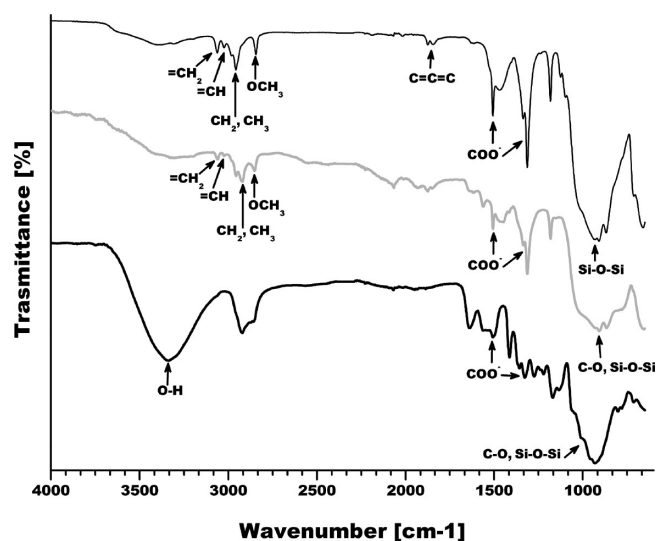

Figure 6. FTIR spectrum of the Zr_6/VTMS/BPO copolymer (thin black line), surface fragment of the wood coated with Zr_6/VTMS/BPO (gray line), inner fragment of the wood coated with Zr_6/VTMS/BPO (bold black line).
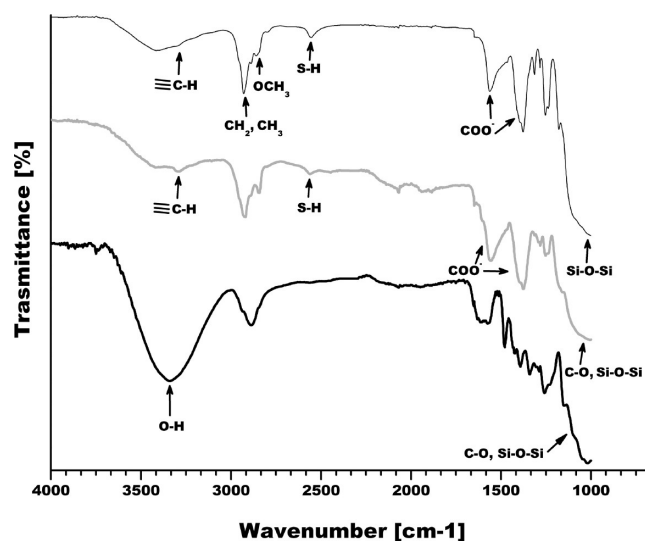

Figure 7. FTIR spectrum of the Zr_6/MPTMS/BPO copolymer (thin black line), surface fragment of the wood coated with Zr_6/MPTMS/BPO (gray line), inner fragment of the wood coated with Zr_6/MPTMS/BPO (bold black line).

and 0.83 for Zr_6/MPTMS/BPO, Figure 10), highlighting that the copolymers were stable and probably would not vary with age. Both DC values were higher than the DC calculated for the copolymers in bulk.[33]

The water static and vibrationally induced equilibrium (VIECA) contact angles, measured on the surface of the

coated wood samples, are shown in Table 3. For each series of samples, six measurements of water static and equilibrium contact angles were performed in different points of the surface. In accord with what was expected, the static contact angles, which are a measurement of the most hydrophobic domains of
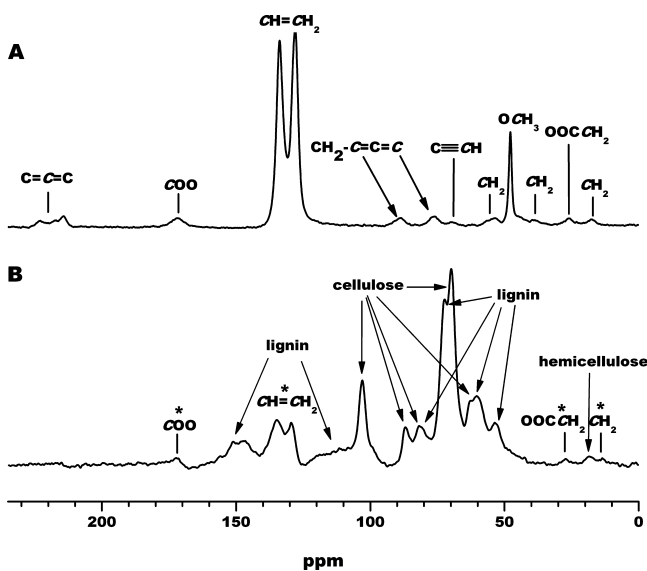
Figure 8. ^{13}C MAS NMR of (A) the copolymer Zr$_6$/VTMS/BPO and (B) fragments of the wood coated with Zr$_6$/VTMS/BPO; * = peaks assigned to the copolymer.
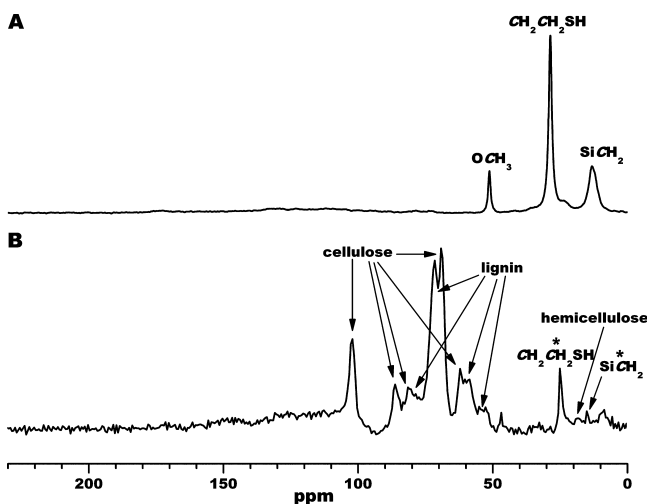
Figure 9. ^{13}C MAS NMR of (A) the copolymer Zr$_6$/MPTMS/BPO and (B) fragments of the wood coated with Zr$_6$/MTMS/BPO; * = peaks assigned to the copolymer.

the surface, were higher compared to the equilibrium contact angles, which provided a value closer to the Young angle.

The water static contact angles were recorded about 10−15 s after the deposition of the drop. Because of the high hydrophilic surface of the untreated wood, neither water equilibrium or static contact angles could be measured. However, from the literature, the water static contact angle registered for untreated pine sapwood after a time of 8 s was about 19°.[63]

For all the wood coated samples, the static and equilibrium contact angles did not exceed 90°, the limit above which a surface is considered hydrophobic, and for this reason, no further investigation on the advancing and receding contact angles of the samples was performed in order to determine the wettability of the surfaces.

Series I presented the highest contact angle values, whereas series III presented the lowest values. The presence of the hydrophilic SH groups in the Zr$_6$/MPTMS/BPO copolymer
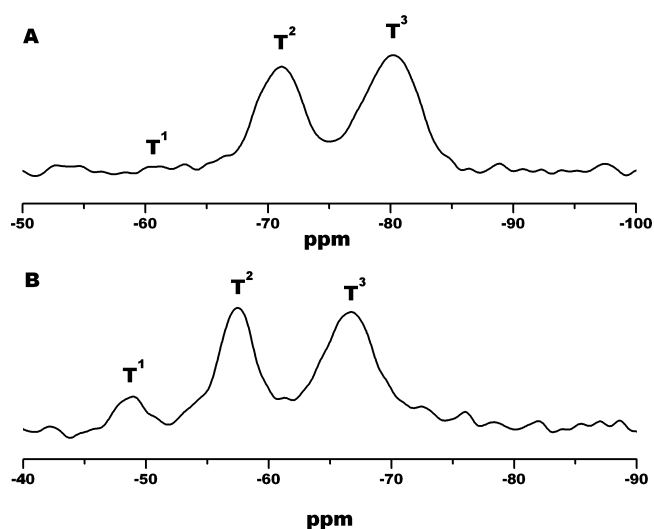
Figure 10. ^{29}Si MAS NMR of the wood samples coated with (A) Zr$_6$/VTMS/BPO and (B) Zr$_6$/MPTMS/BPO.

Table 3. Water Static and Equilibrium Contact Angles

series	θ_{static} (deg)^a	θ_{equil} (deg)^a
I	80 ± 2	73 ± 2
III	51 ± 8	39 ± 6
IV	71 ± 8	59 ± 3

^{a}The contact angles were measured with the aid of a digital camera and the images were analyzed by assuming a spherical approximation of the drop. The equilibrium contact angles were measured using the VIECA (vibrationally induced equilibrium contact angle) method.

was considered to influence the low contact angles recorded for series III.

Although for series I the coating was homogeneously distributed on the surface (low standard deviation), for series III and IV, an inhomogeneous distribution was observed. For series IV, this was explained by considering that the methacrylic ester of thymol was applied on the surface of the sample analyzed by brushing. Instead, for series III the low polymerization level of Zr$_6$/MPTMS/BPO was considered responsible for the lack of homogeneity of the coating. The hypothesis was confirmed by the results of the treatment at 140 °C for 1 h of the sample of series III, which showed higher water static (72° ± 4) and equilibrium (64° ± 3) contact angles with reduced standard deviations.

The results of the biological tests, expressed as the mean dry mass loss percentage values are reported in Table 4 and Figure 12.

At the end of the test, all samples (both treated and control) were completely covered by the mycelium. Nevertheless, the wood samples coated with Zr$_6$/VTMS/BPO (series I and II) had not decayed after 8 weeks; not showing any sign of decay to the naked eye, such as deformation or brown spots on the wood surface. The mean dry mass loss percentage was -1.5 % for series I and -1.8 % for series II, while the mass loss percentage for the control samples was around 60 %. The negative values obtained were probably caused by residual water entrapped beneath the coating during the test. The similar results found for series I and II implies no difference between the mono and double layer coated samples. Therefore, the diverse number of thermal treatments and the difference in

Table 4. Biological Test against *C. puteana*[a]

series	coating	no. of samples	ML %$_{sample}$	no. of controls	ML %$_{control}$
I	Zr$_6$/VTMS/BPO (mono layer)	4	0[b]	3	65 ± 1
II	Zr$_6$/VTMS/BPO (double layer)	4	0[b]	3	62 ± 1
IIIA	Zr$_6$/MPTMS/BPO	8	0	4	31 ± 1
IIIB	Zr$_6$/MPTMS/BPO		16–20		
IVA	Zr$_6$/MPTMS/BPO+ thymol ester	8	0	4	15 ± 1
IVB	Zr$_6$/MPTMS/BPO+ thymol ester		13–20		

[a]IIIA and IVA = samples of series III and IV that did not decay; IIIB and IVB = samples of series III and IV that decayed. [b]Actual values showed a slight mass gain (1.5 and 1.8%).

the amount of copolymer was not a determining factor for the coating performance.

The Zr$_6$/VTMS/BPO polysiloxane matrixes and wood interactions change the physical-chemical properties of the biopolymers making the wood more resistant to biological decay. However, since in our case the amount of copolymer inside the wood was minimal, the positive results obtained with Zr$_6$/VTMS/BPO could be better explained by its capacity to seal the empty space and to eventually reach a smooth continuous surface.

The formation of a barrier against micro-organism penetration and the diminishing of the porosity are extremely important factors for coating without additional biocides since the uptake of fungal metabolites capable of degrading the wood cell components is reduced or prevented.

Coated wood samples of series III and IV presented contrasting results. After 6 weeks, half of the samples of the series still resisted decay (referred to as IIIA and IVA, ML% =
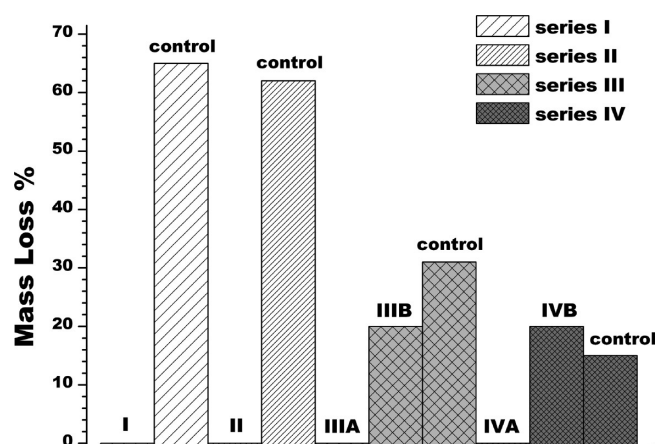

Figure 12. Mass loss percentage of the samples of the four series recovered after the biological test against *C. puteana*. Half of the samples of series III and IV decayed (suffix B) and half did not (suffix A).

0), the other half did not (referred to as IIIB and IV B, see Table 4 and Figure 12). The decayed samples of series III presented a range of dry mass loss percentage (ML% = 13–20%) lower than the control samples (ML% = 31%), while for the decayed samples of series IV (ML% = 15%) there was almost no difference with the control (ML% = 16–20%), leading to suppose a weakened copolymer/wood interaction, probably caused by the reduced availability of SH groups for cross-linking and copolymer wood interaction, because some of the SH group are involved in the bond with the ester of thymol.

FTIR analyses (here not shown) of wood fragments of the samples recovered after the biological test highlighted, for the samples that underwent decay, an increase of the lignin bands at: 1594, 1511, 1424, and 1265 cm^{-1}. This is in accord with a
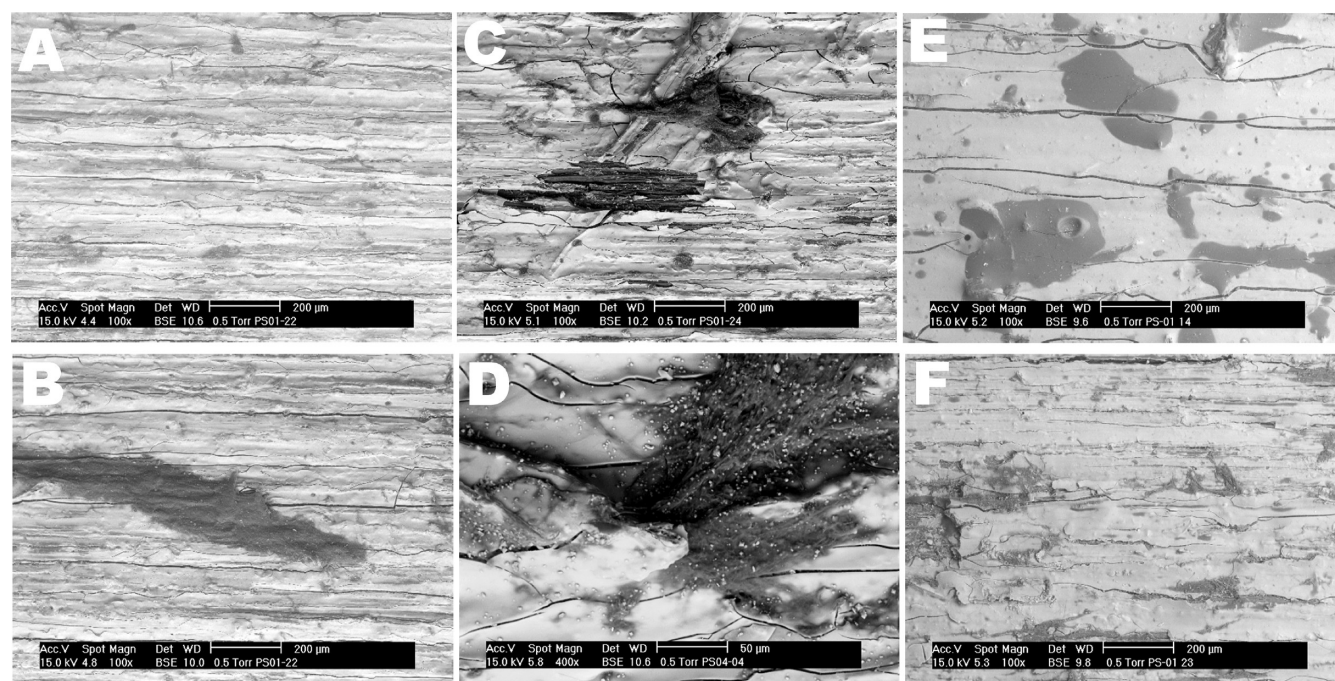

Figure 11. ESEM of the samples recovered after the biological test. A and B = non decayed samples of series III; C and D = decayed samples of series III; E = non decayed sample of series IV; F = decayed sample of series IV. B and D show the action of *C. puteana*, whereas in B, the fungus remained on the surface of the coating, in D, the fungus attacked the wood through a crack of the coating.

Table 5. EDX Analysis Performed on the Surface of the Samples after the Biological Test

series	coating[a]	C %	Si %	Zr %	S %	Si/C	Zr/Si
III	Zr_6/MPTMS/BPO (nd)	85.4 (1.2)	6.3 (0.9)	2.2 (1.5)	6.1 (1.0)	0.074	0.35
III	Zr_6/MPTMS/BPO (d)	87.5 (1.0)	5.4 (1.0)	1.7 (1.7)	5.4 (1.0)	0.062	0.31
IV	Zr_6/MPTMS/BPO + thymol ester (nd)	89.0 (0.9)	5.0 (0.9)	0.7 (2.4)	5.3 (0.9)	0.056	0.14
IV	Zr_6/MPTMS/BPO + thymol ester (d)	87.8 (1.0)	5.5 (0.9)	1.5 (1.7)	3.9 (1.0)	0.063	0.3

[a]d = decayed; nd = not decayed. The values in parentheses are the intensity errors expressed as a percentage of the atomic percentage.

selective attack of C. puteana on the carbohydrate components as should be expected according to the wood decay studies carried with this fungus.[61]

The contrasting results obtained for series III and IV could not be imputed to the different amount of copolymer present on each samples, neither by considering the amount of copolymer initially deposited on the surface nor by the copolymer washed away during the leaching and calculated through the percentage of formulation that leached out (LF%; LF% = 9−22 for series III, LF% = 12−24 for series IV). EDX analysis also did not detect any significant difference in the atomic percentages of the coating components on the surface of the decayed and non-decayed samples (Table 5).

Instead, ESEM analysis showed noticeable dissimilarity in the coatings. A much more cracked surface was observed for the samples that did undergo decay. The yielding of the surfaces could be imputed to the thermal stress suffered from the samples during the sequential steps: leaching and oven drying, carried out before the biological test. The low hydrophobicity of Zr_6/MPTMS/BPO and functionalyzed-Zr_6/MPTMS/BPO could be responsible for the cleavage of these copolymers from the wood. The formation of cracks on the surface allowed the access of the C. puteana to the wood, as was actually observed by several ESEM snapshots (Figure 11D).

From the results obtained for series IV, it was possible to conclude that the ester of thymol did not show an obvious activity against the C. puteana. Even though three of the samples of series IV that resisted to the decay contained a higher amount of ester of thymol (about 0.030 g), the ester was not able to stop the attack of the C. puteana in all the samples of the series. The unavailability of the OH group of the thymol that is locked in the ester could be responsible for the low toxicity. In fact, chemical modification of thymol to various ester derivatives was reported to result in a change in its antibacterial activity.[42] Moreover, the conversion of the thymol into its carbamate derivative was shown to decrease the toxicity towards B. alexandrina, suggesting the necessity of the free hydroxyl group for the maintenance of the toxicity.[64] Similar results were obtained by Veldhuizen et al. on carvacrol, which has an analogous structure of thymol but with the OH in meta position with respect to the methyl group.[65]

4. CONCLUSION

Copolymers Zr_6/VTMS/BPO and Zr_6/MPTMS/BPO were deposited on wood using a modified sol-gel process not involving alkoxysilane pre-hydrolysis. The use of a dip coating wood treatment could explain why the bulk of the coatings remained mainly on the surface of the wood.

Copolymer Zr_6/MPTMS/BPO was successfully post-functionalized by photopolymerizing the free 3-mercaptopropyl groups present in the coating with the methacrylic ester of thymol, which was introduced in order to add a surface-bonded biocide to the copolymer.

An accelerated biological test against C. puteana showed no decay for all the samples treated with Zr_6/VTMS/BPO, while not all the samples treated with Zr_6/MPTMS/BPO resisted decay. The formation of cracks on the surface of some of the samples coated with Zr_6/MPTMS/BPO allowed the fungus access to the wood. The ester of thymol did not show obvious antifungal activity against C. puteana.

Results obtained from biological tests should be considered at a preliminary stage. Supplementary tests by using a higher number of samples, a longer testing period, and different fungal strains could broaden the knowledge on potential applications of these coatings on wood.

Wood pressure impregnation should also be considered for use in future work to increase the impregnation of the wood and thus enhanced its long-term protection. The application of wood pressure impregnation will give also the possibility to better evaluate the ability of the copolymer precursors to penetrate into the wood cell wall.

■ ASSOCIATED CONTENT

Ⓢ Supporting Information

EDX analysis of the copolymers (Zr_6/VTMS/BPO and Zr_6/MPTMS/BPO) and untreated pine sapwood, FTIR and ^{13}C MAS NMR analysis of untreated pine sapwood, ESEM pseudo-topographical analysis of the coated wood samples and untreated pine sapwood, profilometer measurements of the coated wood samples and untreated pine sapwood surfaces, as well as data from the leaching of the coated wood samples. This material is available free of charge via the Internet at http://pubs.acs.org.

■ AUTHOR INFORMATION

Corresponding Author
*E-mail: simonamaggini@gmail.com or simona.maggini@ing.unitn.it. Phone: +39 0461 282415. Fax: +39 0461 281977.

Notes
The authors declare no competing financial interest.

■ ACKNOWLEDGMENTS

■ REFERENCES

(1) Wood Modification: Chemical, Thermal and Other Processes; Renewable Resource; Wiley: Chichester, U.K., 2006.

(2) Trey, S.; Jafarzadeh, S.; Johansson, M. *ACS Appl. Mater. Interfaces* **2012**, *4* (3), 1760.

(3) Trey, S. M.; Netrval, J.; Berglund, L.; Johansson, M. *ACS Appl. Mater. Interfaces* **2010**, *2* (11), 3352.

(4) Mai, C.; Militz, H. *Wood Sci. Technol.* **2004**, *37* (6), 453.

(5) Mai, C.; Militz, H. *Wood Sci. Technol.* **2004**, *37* (5), 339.

(6) Mahltig, B.; Swaboda, C.; Roessler, A.; Böttcher, H. *J. Mater. Chem.* **2008**, *18*, 3180.

(7) Cookson, L. J.; Scown, D. K.; McCarthy, K. J.; Chew, N. *Holzforschung* **2007**, *61*, 326.

(8) Donath, S.; Militz, H.; Mai, C. *Wood Sci. Technol.* **2004**, *38*, 555.

(9) Unger, B.; Bücker, M.; Reinsch, S.; Hübert, T. *Wood Sci. Technol.*, DOI 10.1007/s00226-012-0486-7.

(10) Saka, S.; Sasaki, M.; Tanahashi, M. *Mokuzai Gakkaishi* **1992**, *38*, 1043.

(11) Ogiso, K.; Saka, S. *Mokuzai Gakkaishi* **1993**, *39*, 301.

(12) Schmalzl, K. J.; Evans, P. D. *Polym. Degrad. Stab.* **2003**, *82* (3), 409.

(13) Pandey, K. K.; Chaohan, S. S.; Aggarwal, P. K. *Eur. J. Wood Prod.* **1998**, *56* (6), 412.

(14) Feist, W. C.; Williams, R. S. *Forest Prod. J.* **1991**, *41* (1), 8.

(15) Evans, P. D.; Michell, A. J.; Schmalzl, K. *J. Wood Sci. Technol.* **1992**, *26* (2), 151.

(16) Sun, Q.; Lu, Y.; Zhang, H.; Yang, D.; Wang, Y.; Xu, J.; Tu, J.; Liu, Y.; Li, J. *J. Mater. Sci.* **2012**, *47*, 4457.

(17) Saka, S.; Yakake, Y. *Mokuzai Gakkaishi* **1993**, *39*, 308.

(18) Miyafuji, H.; Saka, S. *Wood Sci. Technol.* **1997**, *31*, 449.

(19) Hübert, T.; Unger, B.; Bücker, M. *J. Sol—Gel Sci. Technol.* **2010**, *53*, 384.

(20) Sun, Q.; Yu, H.; Liu, Y.; Li, J.; Lu, Y.; Hunt, J. F. *Holzforschung* **2010**, *64*, 757.

(21) Tshabalala, M. A.; Sung, L.-P. *J. Coat. Technol. Res.* **2007**, *4* (4), 483.

(22) Tshabalala, M. A.; Libert, R.; Sutherland, N. R. Outdoor Weathering of Sol—Gel-Treated Wood. In *Proceedings of Third International Coating Wood and Wood Composites Conference: Durable and Sustainable—Today and Beyond*; Charlotte, NC, Sept 22—23, 2009 ; National Paint & Coatings Assocation: Washington, D.C., 2009; Vol 1.

(23) Denes, A. R.; Young, R. A. *Holzforschung* **2005**, *53*, 632.

(24) Girardi, F.; Maggini, S.; Della Volpe, C.; Cappelletto, E.; Mueller, K.; Siboni, S.; Di Maggio, R. *J. Sol-Gel Sci. Technol.* **2011**, *60* (3), 315.

(25) Schubert, U.; Hüsing, N.; Lorenz, A. *Chem. Mater.* **1995**, *7*, 2010.

(26) Gross, S. *J. Mater. Chem.* **2011**, *21*, 15853.

(27) Gross, S.; Müller, K. *J. Sol—Gel Sci. Technol.* **2011**, *60* (3), 283.

(28) Di Maggio, R.; Dirè, S.; Callone, E.; Girardi, F.; Kickelbick, G. *J. Sol—Gel Sci. Technol.* **2008**, *48* (1-2), 168.

(29) Heitner, C. Light-Induced Yellowing of Wood-Containing Papers. In *Proceeding of Photochemistry of Lignocellulosic Materials*; San Francisco, April 5—10, 1992 ; Heitner, C., Scaiano, J.C., Eds.; ACS Symposium Series; American Chemical Society: Washington, D.C., 1993; Vol. *531*, Chapter 1, pp 2—25.

(30) Cook, C. M.; Pan, X.; Ragauskas, A. J. *J. Wood Chem. Technol.* **1996**, *16* (3), 327.

(31) Wan, J. K. S.; Depew, M.C. *Res. Chem. Intermed.* **1996**, *22* (3), 241.

(32) Hammel, K.E.; Kapich, A.N.; Jensen, K.A.; Ryan, Z.C. *Enzyme Microb. Technol.* **2002**, *30*, 445.

(33) Maggini, S; Cappelletto, E.; Di Maggio, R. *J. Appl. Polym. Sci.* **2012**, in press, DOI: 10.1002/app.37940.

(34) Maggini, S.; Girardi, F.; Müller, K.; Di Maggio, R. *J. Appl. Polym. Sci.* **2012**, *124*, 2110.

(35) Clausen, C. A.; Woodward, B. M.; Yang, V. W. *Antifungal Essential Oil Metabolites. IRG/WP 10-30531*; International Research Group on Wood Protection: Stockholm, Sweden, 2010; p 9.

(36) Numpaque, M. A.; Oviedo, L. A.; Gil, J. H.; García, C. M.; Durango, D. L. *Trop. Plant Pathol.* **2011**, *36* (1), 3.

(37) Voda, K.; Boh, B.; Vrta-cnik, M.; Pohleven, F. *Int. Biodeterior. Biodegrad.* **2003**, *51*, 51.

(38) Wattanasatcha, A.; Rengpipat, S.; Wanichwecharungruang, S. *Int. J. Pharm.* DOI:10.1016/j.ijpharm.2012.06.017.

(39) Espana, J. M.; Fages, E.; Moriana, R.; Boronat, T.; Balart, R. *Polym. Compos.* **2012**, *33* (8), 1288.

(40) Ramos, M.; Jimenez, A.; Peltzer, M.; Garrigos, M. C. *J. Food Eng.* **2012**, *109* (3), 513.

(41) Moszner, N.; Salz, U.; Rheinberger, V. *Polym. Bull.* **1994**, *33* (1), 7.

(42) Mathela, C. S.; Singh, K. K.; Gupta, v. K. *Acta Polym. Pharm. Drug Res.* **2010**, *67* (4), 375.

(43) Burt, S. *Int. J. Food Microbiol.* **2004**, *94* (3), 223.

(44) Tripti, S.; Adya, P. S. *Wood Sci. Technol.* **2012**, *46* (5), 851.

(45) El Ajjouri, M.; Ghanmi, M.; Satrani, B.; Amarti, F.; Rahouti, M.; Aafi, A.; Ismaili, My R.; Farah, A. *Acta Bot. Gallica* **2010**, *157* (2), 285.

(46) El Ajjouri, M.; Satrani, B.; Ghanmi, M.; Aafi, A.; Farah, A.; Rahouti, M.; Amarti, F.; Aberchane, M. *Biotechnol. Agron. Soc. Environ.* **2008**, *12* (4), 345.

(47) Marin De Mateo, M.; Gonzalez Mateos, F.; Gonzalez Rivas, F. *Antibacterial and fungicidal additives in polymer granulate carriers and/or inorganic agglomerates.* PCT Int. Appl. WO 2012032206 A1 20120315, 2012.

(48) Konuma, R.; Miyazaki, I.; Iida, T.; Hamano, T.; Kawarada, K.; Inoue, M. *Combined antifungal agent compositions, antifungal treatment method, and wood and wood products treated with them.* Jpn. Kokai Tokkyo Koho JP 2011126817 A 20110630, 2011.

(49) Pinto, E.; Pina-vaz, c.; Salgueiro, L.; Concalves, M.J.; de Oliveira, C.; Cavaleiro, C.; Palmeira, A.; Rodrigues, A.; de Oliveira, J.M. *J. Med. Microbiol.* **2006**, *55*, 1367.

(50) Panov, D.; Terziev, N. *Int. Biodeterior. Biodegrad.* **2009**, *63*, 456.

(51) Donath, S.; Militz, H.; Mai, C. *Holzforschung* **2006**, *60* (2), 210.

(52) Ghosh, S. C.; Militz, H.; Mai, C. *BioResources* **2008**, *3* (4), 1303.

(53) Hook, R. J. *J. Non-Cryst. Solids* **1996**, *195*, 1.

(54) Della Volpe, C.; Maniglio, D.; Morra, M.; Siboni, S. *Colloids Surf., A* **2002**, *206*, 46.

(55) Della Volpe, C.; Maniglio, D.; Siboni, S.; Morra, M. *Oil Gas Sci. Technol.* **2001**, *56*, 9.

(56) *EN 84:1997. Wood Preservatives—Accelerated Aging of Treated Wood Prior to Biological Testing. Leaching Procedure.* European Committee for Standardization: Brussels, Belgium, 1997.

(57) Bravery, A. F. *IRG/WP 2113. A Miniaturized Wood Block for the Rapid Evaluation of Wood Preservative Fungicides*; International Research Group on Wood Protection: Stockholm, Sweden, 1978

(58)) *EN 113:1996. Wood Preservatives. Test Method for Determining the Protective Effectiveness against Wood Destroying Basidiomycetes—Determination of the Toxic Values*; European Committee for Standardization: Brussels, Belgium , 1996.

(59) Di Maggio, R.; Dire', S.; Callone, E.; Girardi, F.; Kickelbick, G. *Polymer* **2010**, *51*, 832.

(60) Di Maggio, R.; Callone, E.; Girardi, F.; Dire', S. *J. Appl. Polym. Sci.* **2012**, *127* (3), 1713.

(61) Pandey, K .K.; Pitman, A.J. *Int. Biodeterior. Biodegrad.* **2003**, *52*, 151.

(62) Bardet, M.; Gerbaud, G.; Giffard, M.; Doan, C.; Hediger, S.; Le Pape, L. *Prog. Nucl. Magn. Reson. Spectrosc.* **2009**, *55*, 199.

(63) Boehme, C.; Hora, G. *Holzforschung* **1996**, *50*, 269.

(64) Radwan, M. A.; El-Zemity, S. R.; Mohamed, S. A.; Sherby, S. M. *Ecotoxicol. Environ. Safety* **2008**, *71*, 889.

(65) Veldhuizen, E. J.; Tjeerdsma-van Bokhoven, J. L.; Zweijtzer, C.; Burt, S. A.; Haagsman, H. P. *J. Agric. Food Chem.* **2006**, *54* (5), 1874.